

# NTAL phosphorylation is a pivotal link between the signaling cascades leading to human mast cell degranulation following Kit activation and FcεRI aggregation

Christine Tkaczyk, Vaclav Horejsi, Shoko Iwaki, Petr Draber, Lawrence E. Samelson, Anne B. Satterthwaite, Dong-Ho Nahm, Dean D. Metcalfe, and Alasdair M. Gilfillan

**Aggregation of high-affinity receptors for immunoglobulin E (FcεRI) on the surface of mast cells results in degranulation, a response that is potentiated by binding of stem cell factor (SCF) to its receptor Kit. We observed that one of the major initial signaling events associated with FcεRI-mediated activation of human mast cells (HuMCs) is the rapid tyrosine phosphorylation of a protein of 25 to 30 kDa. The phosphorylation of this protein was also observed in response to SCF. This protein was identified as non-T-cell activa-**

**tion linker (NTAL), an adaptor molecule similar to linker for activated T cells (LAT). Unlike the FcεRI response, SCF induced NTAL phosphorylation in the absence of detectable LAT phosphorylation. When SCF and antigen were added concurrently, there was a marked synergistic effect on NTAL phosphorylation, however, SCF did not enhance the phosphorylation of LAT induced by FcεRI aggregation. FcεRI- and SCF-mediated NTAL phosphorylation appear to be differentially regulated by Src kinases and/or Kit**

**kinase, respectively. Diminution of NTAL expression by silencing RNA oligonucleotides in HuMCs resulted in a reduction of both Kit- and FcεRI-mediated degranulation. NTAL, thus, appears to be an important link between the signaling pathways that are initiated by these receptors, culminating in mast cell degranulation. (Blood. 2004;104:207-214)**

© 2004 by The American Society of Hematology

## Introduction

Mast cell activation leading to degranulation, arachidonic acid metabolism, and cytokine production is initiated following antigen-dependent aggregation of high-affinity receptors for immunoglobulin E (IgE) (FcεRI) on the cell surface.<sup>1</sup> Stem cell factor (SCF), although primarily required for the growth, differentiation, and survival of mast cells by binding to Kit,<sup>2,3</sup> potentiates secretory responses elicited via the FcεRI.<sup>4</sup> Both FcεRI and Kit responses follow tyrosine kinase activation and subsequent protein tyrosine phosphorylation.<sup>5,6</sup> FcεRI possess no inherent tyrosine kinase activity thus require the recruitment of the *Src* family tyrosine kinase, Lyn, and the zeta-associated protein 70 (ZAP 70)-related tyrosine kinase, spleen tyrosine kinase (Syk), into the signaling complex, where, following receptor aggregation, they become sequentially activated.<sup>7,8</sup> Subsequent tyrosine phosphorylation of the β and γ chains of the FcεRI, and of the transmembrane adaptor molecule linker for activated T cells (LAT), provides multiple docking sites for downstream Src homology 2 (SH2) domain-containing signaling molecules.<sup>9</sup> These initial tyrosine-phosphorylation events appear to be crucial for subsequent FcεRI-mediated degranulation to proceed.

Unlike the FcεRI, Kit does possess inherent tyrosine kinase activity.<sup>10,11</sup> Binding of SCF induces autophosphorylation of Kit

with consequential binding of SH2 domain-containing signaling molecules to the Kit cytosolic domain.<sup>12</sup> In contrast to FcεRI signaling, to date there is little evidence that LAT or similar transmembrane adaptor molecules become phosphorylated following Kit activation. Thus, despite, Kit's ability to potentiate FcεRI-mediated degranulation, there is little indication as to how the immediate signaling events initiated by Kit may be integrated into those initiated following FcεRI aggregation. We therefore examined the early protein tyrosine-phosphorylation events following activation of human mast cells via both FcεRI and Kit to determine whether these receptors shared common early signaling steps.

Using optimized extraction conditions to examine early protein tyrosine-phosphorylation signaling in FcεRI-activated human mast cells (HuMCs),<sup>13</sup> we observed that one of the major early responses was the tyrosine phosphorylation of a small-molecular-weight (MW) protein of approximately 25 to 30 kDa (p30). In this report, we now show that this protein is also phosphorylated following Kit activation; describe the identification of this protein as the transmembrane adaptor molecule, non-T-cell activation linker (NTAL)<sup>14,15</sup>; and present data that support the concept that NTAL phosphorylation is a pivotal step in the signaling pathways leading to degranulation following FcεRI aggregation and Kit activation.

From the Laboratory of Allergic Diseases, National Institute of Allergy and Infectious Diseases (NIAID), National Institutes of Health, Bethesda, MD; the Institute of Molecular Genetics, Academy of Sciences of the Czech Republic, Prague, Czech Republic; the Laboratory of Cellular and Molecular Biology, Center for Cancer Research, National Cancer Institute, National Institutes of Health, Bethesda MD; and the Department of Internal Medicine and Center for Immunology, University of Texas Southwestern Medical Center, Dallas, TX.

Submitted August 12, 2003; accepted March 2, 2004. Prepublished online as *Blood* First Edition Paper, March 9, 2004; DOI 10.1182/blood-2003-08-2769.

Supported by the NIAID Intramural Program and by the Center of Molecular and Cellular Immunology (LN00A026), Ministry of Education, Youth and Sports of the Czech Republic (V.H. and P.D.). The research of P.D. was also supported

by an International Research Scholar's award from Howard Hughes Medical Institute. A.B.S. is the Southwestern Medical Foundation Scholar in Biomedical Research.

**Reprints:** Alasdair M. Gilfillan, Laboratory of Allergic Diseases, National Institute of Allergy and Infectious Diseases, National Institutes of Health, Building 10, Room 11C206, 10 Center Dr, MSC 1881, Bethesda, MD 20892-1881; e-mail: agilfillan@niaid.nih.gov.

The publication costs of this article were defrayed in part by page charge payment. Therefore, and solely to indicate this fact, this article is hereby marked "advertisement" in accordance with 18 U.S.C. section 1734.

© 2004 by The American Society of Hematology

## Materials and methods

### Cell culture

HuMCs,<sup>16</sup> RBL 2H3 cells,<sup>7</sup> mouse bone marrow–derived mast cells (BMMCs),<sup>17</sup> and the human monocytic U937 cell<sup>18</sup> line were cultured as detailed. The *Lyn*<sup>-/-</sup> and Bruton tyrosine kinase (*Btk*)<sup>-/-</sup> mice used in this study have been previously described.<sup>19</sup>

### Cell activation

HuMCs were sensitized with 4-hydroxy-3-nitrophenylacetyl-(NP)-specific chimeric mouse F(ab), human Fc-IgE (NP-IgE, 1000 ng/mL; Serotec, Raleigh, NC), and then activated with 4-hydroxy-3-nitrophenylacetyl-bovine serum albumin conjugate (NP-BSA, 0-100 ng/mL, 0 to 1800 seconds; Biosearch Technologies, Novato, CA) as reported.<sup>13</sup> Cells were generally stimulated for longer than 30 seconds or, as indicated in the figure legends, to reduce the margin of error of sampling. Mouse BMMCs were sensitized with mouse monoclonal anti-dinitrophenyl (DNP) IgE (1000 ng/mL; Sigma, St Louis, MO) and triggered with DNP–human serum albumin (HSA) conjugate (100 ng/mL; Sigma). Secretion was monitored by  $\beta$ -hexosaminidase ( $\beta$ -hex) release.<sup>20</sup>

For activation of Kit, HuMCs were cultured with Stem Pro media without cytokines for 12 to 16 hours prior to conducting the experiments. These conditions did not markedly influence Fc $\epsilon$ RI-mediated signaling responses, including phospholipase C  $\gamma_1$  (PLC $\gamma_1$ ) phosphorylation, inositol phosphate production, phosphatidylinositol 3 (PI-3) kinase activation, calcium mobilization, and tyrosine phosphorylation, compared with the responses observed in nondeprived HuMCs (data not shown). When the responses obtained with SCF in the presence of Fc $\epsilon$ RI aggregation were examined and for experiments using short-interfering RNA (siRNA), NP-IgE (100 ng/mL) was included in the culture media during the 12 to 16 hours prior to conducting the experiments. Cells were then triggered by the addition of SCF (100 ng/mL; Pepro Tech, Rocky Hill, NJ) and/or NP-BSA (100 ng/mL). In experiments in which the effects of inhibitors were examined, these compounds were added 10 minutes prior to the addition of NP-BSA.

### Antibodies and immunoblot analysis

Mouse monoclonal antibodies (mAbs; NAP-05, NAP-07, and NAP-08), and the rabbit polyclonal antibody (pAb) against amino acids 89-243 of human NTAL were produced in the laboratory of V.H.<sup>14</sup> Antiphosphotyrosine mAb (4G10), anti-Syk mAb (4D10), and anti-phospho-LAT (pY<sup>191</sup>) pAb were obtained from UBI (Lake Placid, NY). Anti-LAT mAb was produced in the laboratory of P.D., and anti-LAT pAb was from the laboratory of L.E.S. Anti-phospho-PLC $\gamma_1$  (pY<sup>783</sup>) pAb, anti-phospho-Kit (pY<sup>568-570</sup>) pAb, and anti-phospho-Kit (pY<sup>823</sup>) pAb were obtained from Biosource (Camarillo, CA). Anti-phospho-AKT (pS<sup>473</sup>) pAb was obtained from Cell Signaling Technology (Beverly, MA).

Cell lysates were prepared and proteins separated as described and then probed with indicated antibodies and visualization of immunoreactive proteins by enhanced chemiluminescence (ECL; NEN, Boston, MA).<sup>13</sup> To accurately assess MWs of phosphorylated molecules, the proteins were separated on 14% Tris (tris(hydroxymethyl)aminomethane)-glycine gels (Invitrogen, Frederick, MD).

### Immunoprecipitation studies

HuMCs were lysed at 4°C by the addition of equal volumes of Tris-buffered saline (TBS) containing nonidet P-40 (NP-40; 1%) and octyl- $\beta$ -glucoside (60 mM). The suspensions were incubated on ice for 30 minutes, and then the cell debris was removed by centrifugation at 20 400g for 15 minutes at 4°C. NTAL and LAT antibodies were coupled to protein G–sepharose beads (Amersham Biosciences, Piscataway, NJ) and incubated with the cell lysates by rotating for either 3 hours at room temperature or 12 hours at 4°C. NTAL was immunoprecipitated from mouse BMMCs with anti-NTAL

mAbs. Due to higher efficiency of capture with the pAb, however, the anti-NTAL pAb was used for immunoprecipitation of NTAL from HuMCs.

For protein normalization, gels were either stripped and then reprobed or identically loaded samples were probed with anti-Syk antibody and anti-LAT or anti-NTAL antibodies as described in the figure legends. In these blots, Syk was routinely recognized as a doublet reflecting the differently spliced isoforms.<sup>21</sup>

### RNA silencing

RNA silencing studies were conducted essentially as described by Janssen et al,<sup>15</sup> however, oligonucleotides were redesigned based on the human sequence. Briefly, 3 different 21-mer siRNA duplexes for human NTAL and LAT were designed and purchased from Dharmacon (Boulder, CO) on the basis of the following target sequences for (a) NTAL: 5'-AACAAAGCT-GTTGCAATTCTAC-3', 5'-AAGGTACCAGAACTTCAGCAA-3', and 5'-AAGATGATGATGCCAATTCCT-3'; and (b) LAT: 5'-AACAGCA-CATCCTCAGATAGT-3', 5'-AAGTGTGGCGAGCTACGAGAA-3', and 5'-AATGAGGACGACTATCACAAC-3'.

The following green fluorescent protein (GFP) target sequence for siRNA was used as a negative control: 5'-GGC TAC GTC CAG GAG CGC ACC-3'. The duplexes were synthesized with 2 residues Thymidine in 3' overhang (dTdT).

The oligonucleotides (20  $\mu$ M) were preincubated in 3  $\mu$ L oligofectamine (Invitrogen) for 15 minutes at room temperature, and then the 3 double-stranded RNAs (dsRNAs; + oligofectamine) for NTAL or LAT were added to HuMCs in Stem Pro medium ( $0.3 \times 10^6$  cells/mL) containing cytokines but no antibiotics. The cells (3 mL/well) were incubated for 48 hours at 37°C. At this point, the cells were washed, transferred to new wells, and then incubated for a further 16 hours with fresh oligonucleotides and sensitized with IgE as described for cell activation. For negative controls, the cells were incubated in identical volumes of oligofectamine with or without GFP siRNA.

### Data presentation

Unless otherwise stated, the data are means  $\pm$  SE of the indicated number of experiments conducted in duplicate. Statistical comparisons were conducted by 2-tailed *t* test for paired samples using Prism software (GraphPad Software, San Diego, CA).

## Results

### Tyrosine phosphorylation of a major small-MW protein in HuMCs following Fc $\epsilon$ RI aggregation and Kit activation

We first examined the early Fc $\epsilon$ RI- and Kit-dependent protein tyrosine-phosphorylation events in HuMCs. When sensitized with NP-IgE, NP-BSA–induced Fc $\epsilon$ RI aggregation resulted in a concentration-dependent (Figure 1A) and, as previously demonstrated,<sup>13</sup> time-dependent (Figure 1B) increase in tyrosine phosphorylation of multiple protein substrates. The major response was the tyrosine phosphorylation of proteins between 72 and 76 kDa, which has been described to contain hematopoietic specific protein 1 (HS1),<sup>22</sup> Syk,<sup>7</sup> and SH2 domain–containing leukocyte protein of 76 kDa (SLP-76)<sup>23</sup> in RBL 2H3 cells and mouse BMMCs. Secondary only to this response was the marked tyrosine phosphorylation of a protein with an apparent MW of 25 kDa (Figure 1A-B). Subsequent accurate determination on linear gels revealed a MW of 29 to 30 kDa (p30). The phosphorylation of p30 maximized within 30 seconds following Fc $\epsilon$ RI aggregation and concentrations of NP-BSA between 1 and 10 ng/mL. These parameters closely correlated with the concentration requirements of antigen (Figure 1C) and kinetics (Figure 1D) for the degranulation of HuMCs.

To examine SCF responses, HuMCs were cultured overnight in the absence of growth factors, as described in “Materials and

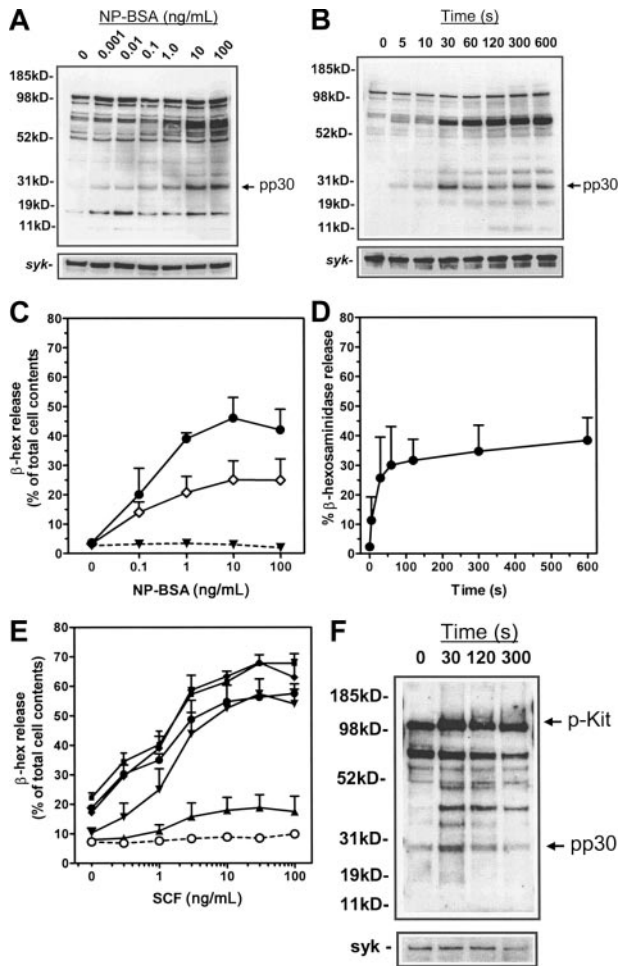


**Figure 1. Protein tyrosine phosphorylation in HuMCs and degranulation following FcεRI aggregation and SCF challenge.** Total cellular protein phosphorylation was assessed in panels A-B by sensitizing HuMCs overnight with 1000 ng/mL NP-IgE, and then triggering for 5 minutes with (A) the indicated concentrations of NP-BSA or (B) 100 ng/mL NP-BSA for the indicated periods of time. Membranes were probed with an antiphosphotyrosine antibody. (C-D) For degranulation experiments, HuMCs were sensitized overnight with either 1000 ng/mL (●) or 100 ng/mL (○) NP-IgE and then triggered for 30 minutes (C) with the indicated concentrations of NP-BSA or (D) with NP-BSA (100 ng/mL) for the indicated periods of time. ▼ indicates no sensitization. (E) HuMCs were cultured overnight in the absence of SCF but in the presence of NP-IgE (100 ng/mL). The cells were then challenged with SCF either in the absence (○) or presence of NP-BSA: (▲), 0.01 ng/mL; (▼), 0.1 ng/mL; (◆), 1 ng/mL; (■), 10 ng/mL; and (●), 100 ng/mL. (F) HuMCs were challenged for the indicated times with SCF (100 ng/mL) in the absence of NP-BSA prior to probing for phosphotyrosine as described in "Materials and methods." The degranulation experiments are means ± SEM of n = 2 to 5 experiments conducted in duplicate, and the blots are representative of at least n = 3.

methods," then challenged with SCF in the absence of antigen. This had little effect on degranulation (Figure 1E). To then examine the ability of SCF to potentiate FcεRI-mediated degranulation, HuMCs were sensitized with NP-IgE, and then challenged with SCF (0.3-100 ng/mL) in the presence of NP-BSA (0.01-100 ng/mL). Under these conditions, SCF induced a marked concentration-dependent potentiation of FcεRI-mediated degranulation (Figure 1E). Following SCF challenge alone, an increase in tyrosine phosphorylation of a number of proteins was observed (Figure 1F); however, the pattern of phosphorylation was distinctly different from that observed upon FcεRI aggregation (compare 1F with 1B). One major exception was the rapid phosphorylation of p30, which, as described, was also observed following FcεRI aggregation. This response again maximized within 30 seconds of SCF challenge, however, it appeared to be more transient than that observed

following FcεRI aggregation. Occasionally, as in Figures 1F, 5, and 6, we observed a degree of constitutive phosphorylation of p30. This was more evident when blots were overexposed.

**Identification of the tyrosine-phosphorylated 29- to 30-kDa protein (pp30)**

As the phosphorylation of p30 appeared to be one of the major early signaling responses associated with FcεRI-mediated degranulation, and as this response was also elicited by Kit following binding to SCF, we proceeded to identify this molecule. Recently, a novel transmembrane adaptor molecule of 30 kDa, NTAL, was identified in human and mouse B cells, natural killer (NK) cells, and monocytes, and rodent mast cells where it became tyrosine phosphorylated upon FcεRI aggregation.<sup>14</sup> To explore the possibility that p30 was NTAL, we first examined the expression of NTAL in HuMCs compared with U937 cells, RBL 2H3 cells, and mouse BMDCs, using a panel of anti-NTAL mAbs and pAb. All anti-NTAL antibodies recognized human NTAL as a 29- to 30-kDa protein in HuMCs and U937 cells (Figure 2A), however, only the anti-NTAL mAb recognized the rodent NTAL expressed in mouse BMDCs and RBL 2H3. The MW of NTAL in these cells was slightly lower than in HuMCs. The expression and gel migration of LAT was examined as a reference (Figure 2B) in these studies. Anti-LAT mAb and pAb recognized LAT with a MW of approximately 38 kDa in mast cells as expected, but not in U937 cells (Figure 2B).

Comparison of the migration of NTAL to the tyrosine-phosphorylated proteins extracted from antigen-challenged HuMCs and mouse BMDCs demonstrated that, although human and mouse

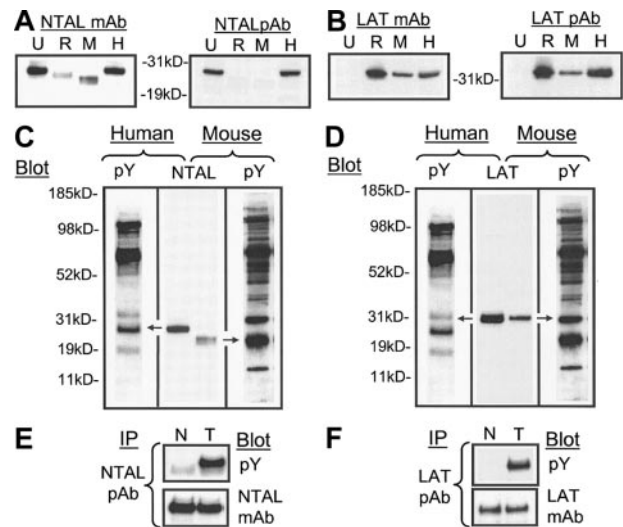


**Figure 2. The expression and tyrosine phosphorylation of NTAL and LAT following FcεRI aggregation in human mast cells.** (A-B) Whole cell lysates (100 000 cell equivalents) of U937 cells (U), RBL 2H3 cells (R), mouse BMDCs (M), and HuMCs (H) were probed with anti-NTAL and anti-LAT monoclonal (m) (NAP 08) and polyclonal (p) antibodies. Comigration of (C) NTAL with pp30 in HuMCs and an equivalent tyrosine-phosphorylated protein in mouse BMDCs and (D) LAT with pp38 in HuMCs and in mouse BMDCs. HuMCs and BMDCs were triggered as described in "Materials and methods" and probed with an antiphosphotyrosine mAb (pY). Extracts as in panels A-B were probed with either an anti-NTAL pAb or anti-LAT mAb (NAP-08), and the gels were then aligned based on the migration of standard molecular-weight markers. (E-F) HuMCs were sensitized and triggered with NP-BSA (100 ng/mL) for 30 seconds (T), and then the phosphorylation was compared with nonactivated cells (N). The lysates were then probed with the indicated antibodies. The proteins in panels A-D were extracted under denaturing conditions and in panels E-F, under the conditions for immunoprecipitation as described in "Materials and methods." IP indicates immunoprecipitation. The data are representative of n = 2 to 3.

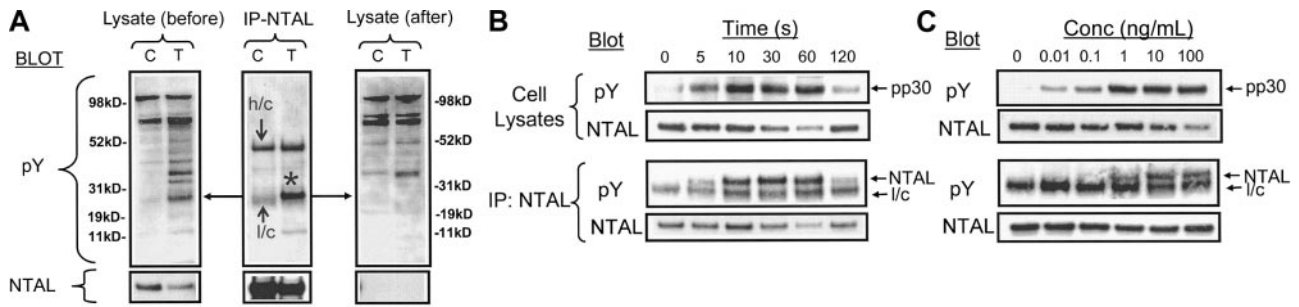


**Figure 3. Characterization of NTAL phosphorylation after FcεRI aggregation in HuMCs.** (A) Immunodepletion of pp30 from HuMCs with anti-NTAL pAb. HuMCs were sensitized and triggered for 60 seconds, and aliquots of the cell lysates were immunoprecipitated using an anti-NTAL pAb as described in "Materials and methods." The immunoprecipitates and aliquots of the lysates before and after immunoprecipitation were then probed with 4G10 antiphosphotyrosine mAb or an anti-NTAL mAb. \*Band for NTAL (B) Comparative kinetics of NTAL and pp30 phosphorylation. In these and other blots, the observed decrease in antibody recognition of NTAL (eg, at 60 seconds) represents epitope masking due to phosphorylation. (C) Comparative concentration dependency of NTAL and pp30 phosphorylation following FcεRI aggregation. The cell lysates were all prepared under nondenaturing conditions as for Figure 2E-F. Conc indicates concentration; l/c, IgG light chain; h/c, IgG heavy chain; pY, phosphotyrosine; and asterisk, phosphorylated NTAL. The blots are representative of 2 to 3 similar experiments.

NTAL migrated to slightly different MWs, NTAL aligned with pp30 in HuMCs, and with a corresponding slightly smaller MW, but still heavily tyrosine phosphorylated, protein in mouse BMMCs (Figure 2C). In comparison, LAT had a higher MW than pp30 (Figure 2D), aligning with a tyrosine-phosphorylated protein of 38 kDa MW. Immunodepletion experiments confirmed that the 38-kDa tyrosine-phosphorylated protein was LAT (data not shown). To next determine whether NTAL was indeed tyrosine phosphorylated upon FcεRI aggregation in HuMCs, and to compare these findings with that of LAT, these molecules were immunoprecipitated from activated HuMCs and then probed with an antiphosphotyrosine antibody. A marked tyrosine phosphorylation of NTAL was observed following FcεRI aggregation (Figure 2E). As expected, LAT was also tyrosine phosphorylated following FcεRI aggregation (Figure 2F).

To confirm that pp30 was phosphorylated NTAL, we conducted immunodepletion studies. HuMCs were challenged with antigen, proteins extracted with NP-40 and octyl-β-glucoside as described in "Materials and methods," and then aliquots were immunoprecipitated with anti-NTAL pAb. The immunoprecipitates and lysates, before and after immunoprecipitation, were then probed with antiphosphotyrosine and anti-NTAL mAbs. From Figure 3A, it can be seen that immunoprecipitation with the anti-NTAL antibody depleted NTAL from the cell lysates. In parallel, there was a marked depletion of pp30 from the lysates following immunoprecipitation with the anti-NTAL pAb. This was associated with immunoprecipitation of a tyrosine-phosphorylated protein corresponding to pp30 in the immunoprecipitates, confirming that pp30 and tyrosine-phosphorylated NTAL were the same molecule. In these studies, however, a slight decrease in intensity of 1 or 2 of the

minor tyrosine-phosphorylated proteins was also observed following immunodepletion of NTAL. These may represent proteins associating with NTAL in vivo or may be due to antibody cross-reactivity. Examination of the kinetics of NTAL phosphorylation (Figure 3B) revealed that this response maximized between 10 to 30 seconds after FcεRI aggregation, and then subsequently decreased in a manner identical to that for pp30 (also see Figure 1). Similarly, maximal phosphorylation of pp30 and NTAL (Figure 3C) was observed at concentrations of NP-BSA between 1 to 10 ng/mL (Figure 3C). Thus, by multiple parameters, phosphorylated NTAL and pp30 are the same molecule.

**Regulation of FcεRI-dependent NTAL phosphorylation**

FcεRI-mediated tyrosine phosphorylation in RBL 2H3 cells is regulated by Lyn and Syk.<sup>24</sup> In addition, PI-3 kinase may also indirectly mediate FcεRI-dependent tyrosine phosphorylation in RBL 2H3 cells.<sup>25</sup> To therefore examine whether these events led to NTAL phosphorylation in HuMCs, we used PP2, piceatannol, and wortmannin, which are inhibitors of *Src* family kinases,<sup>26</sup> Syk,<sup>27</sup> and PI-3 kinase,<sup>25</sup> respectively. In cell lysates, FcεRI-dependent PP2 phosphorylation of the proteins corresponding to both NTAL and LAT was inhibited in a concentration-dependent manner by PP2 (Figure 4A) and by piceatannol (Figure 4B) but not by wortmannin (data not shown). Similarly, immunoprecipitation studies revealed that, at both early time points (10 seconds) and late time points (120 seconds), FcεRI-dependent NTAL phosphorylation was inhibited by PP2 and piceatannol (Figure 4C). In contrast, at early time points following cell activation (10 seconds), wortmannin had no effect on NTAL phosphorylation; however by 120

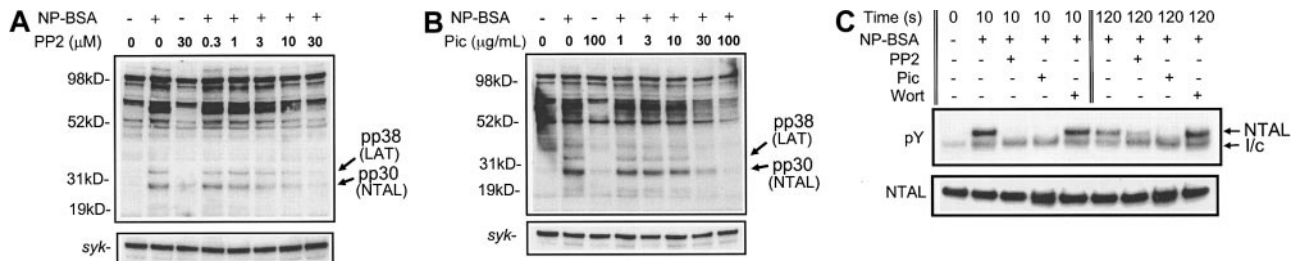


**Figure 4. The effects of the Src kinase inhibitor PP2 and the Syk inhibitor piceatannol on the phosphorylation of pp30 (NTAL) and pp38 (LAT).** PP2 (A), piceatannol (B), or carrier solutions were added 10 minutes prior to the addition of 100 ng/mL NP-BSA. The reactions were terminated after 5 minutes by the addition of denaturing lysis buffer. pic indicates piceatannol. (C) Effect of inhibitors on NTAL phosphorylation. HuMCs were sensitized and triggered as described in the legend for Figure 1C, and NTAL phosphorylation was determined as described in the legend for Figure 3A. The blots are representative of 2 to 3 similar experiments. Wort indicates wortmannin; l/c, IgG light chain; and pY, phosphotyrosine.

seconds, wortmannin potentiated the FcεRI-dependent NTAL phosphorylation observed in the absence of wortmannin at this time point. Taken together these data argue that both *Src* kinases and Syk, but not PI-3 kinase, are required for NTAL phosphorylation.

**Phosphorylation of NTAL by SCF in human mast cells**

From Figure 1F, it appeared that p30 (NTAL) was also phosphorylated following SCF binding to Kit. To confirm this observation, HuMCs deprived of growth factors overnight were challenged with SCF (100 ng/mL) in the absence of antigen; then NTAL and LAT were immunoprecipitated with anti-NTAL and anti-LAT antibodies, and these immunoprecipitates were probed with antiphosphotyrosine mAb. From Figure 5A it can be seen that SCF induced tyrosine phosphorylation of NTAL. Similarly, phosphorylation of NTAL in response to SCF was also observed in mouse BMMCs (Figure 5B-C). In contrast, phosphorylation of LAT in response to SCF was not detected (Figure 5A). However, it is possible that this response was below detection limits.

To facilitate further studies, we used an antibody (anti-(pY<sup>191</sup>)-LAT) that recognized a common tyrosine-phosphorylated epitope in both LAT and NTAL in FcεRI-activated mast cells (Figure 5B). This antibody also recognized phosphorylated recombinant human NTAL (data not shown). Probing lysates of SCF-challenged HuMCs with the anti-(pY<sup>191</sup>)-LAT antibody further confirmed that SCF induced the tyrosine phosphorylation of NTAL in the absence of LAT (Figure 5C). Phosphorylation of NTAL maximized 30 to 60 seconds after challenge and then rapidly declined. These kinetics are identical to those observed for the phosphorylation of pp30 (NTAL) in response to SCF (Figure 1F), however they are somewhat delayed from that observed following FcεRI aggregation (Figure 3B), in which maximal phosphorylation was observed between 10 and 30 seconds following antigen challenge. NTAL phosphorylation in response to SCF appeared concurrently, but

maximized earlier than the phosphorylation of Kit (tyrosines Y<sup>568</sup>, Y<sup>570</sup>, and Y<sup>823</sup>), and preceded the phosphorylation of PLCγ<sub>1</sub> and phosphorylation of AKT, an index of PI-3 kinase activation.

As SCF potentiates FcεRI-mediated degranulation, we examined whether FcεRI-mediated NTAL phosphorylation was similarly potentiated. SCF (100 ng/mL) was added concurrently with NP-BSA to sensitized cells. When examined at an early time point (10 seconds), the response to SCF was less than that observed with antigen; however, when added concurrently, there was a marked potentiation of NTAL phosphorylation (Figure 5D). At a later time point (60 seconds), however, the observed response to SCF was greater than that observed with antigen, and the response of SCF in the presence of antigen had decreased from 10 seconds to a level that was lower than that observed in response to SCF alone. Thus, not only did SCF potentiate FcεRI-mediated NTAL phosphorylation (and/or vice versa), the kinetics of the response were also enhanced. In contrast, SCF had no effect on the phosphorylation of LAT in response to antigen at either 10 seconds or 60 seconds of activation; however, all other signaling responses examined, including phosphorylation of PLCγ<sub>1</sub> and activation of PI-3 kinase as monitored by AKT, were potentiated (Figure 6D). Unexpectedly, although Kit was not phosphorylated following FcεRI aggregation, the phosphorylation of Kit following SCF challenge was substantially potentiated when SCF was added concurrently with antigen.

**The regulation of Kit-mediated NTAL phosphorylation**

To investigate the pathways regulating Kit-mediated NTAL phosphorylation, we next examined the ability of PP2 to block this response. In addition to inhibiting *Src* kinases, PP2 also blocks inherent Kit kinase activity.<sup>28</sup> We therefore initially determined the effect of PP2 on the autophosphorylation of KIT in response to SCF. From Figure 6A, it can be seen that again SCF, but not antigen, induced autophosphorylation of Kit, and that this autophosphorylation was blocked by PP2 at concentrations that have been

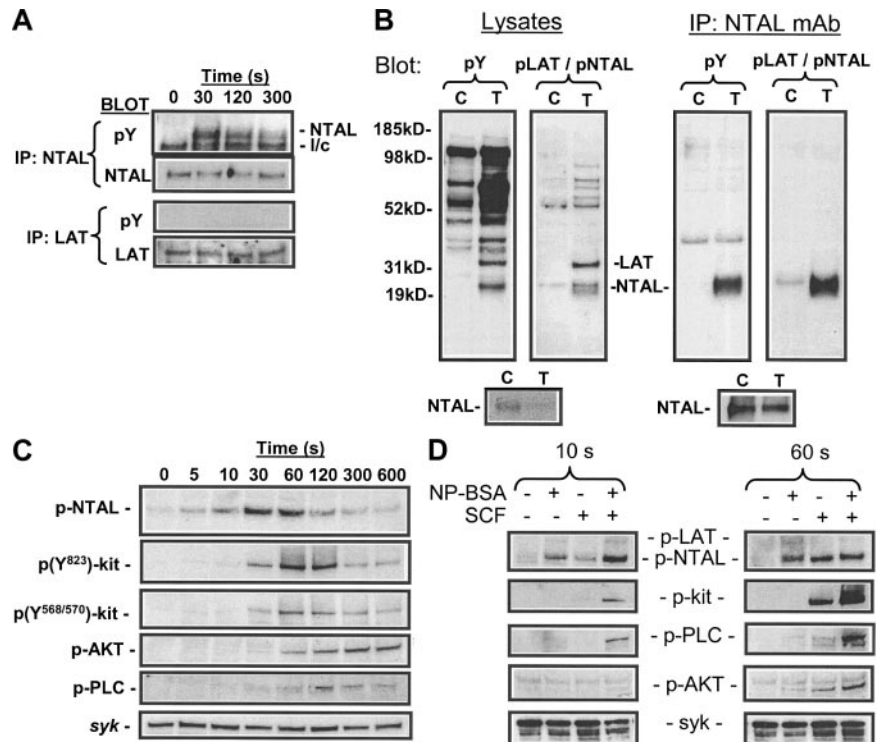


**Figure 5. Phosphorylation of NTAL in response to SCF.** (A) HuMCs were challenged with SCF (100 ng/mL) for the indicated periods of time, and then the proteins were extracted and immunoprecipitated with either an anti-NTAL pAb or an anti-LAT mAb as described in "Materials and methods." The lysates were then probed with an antiphosphotyrosine antibody (pY) or an anti-NTAL mAb or anti-LAT pAb. (B) Recognition of phosphorylated NTAL by anti-pY<sup>191</sup> LAT antibody. Mouse BMMCs were sensitized and then stimulated with antigen for 120 seconds as described in "Materials and methods." Cell lysates and NTAL immunoprecipitates, captured with anti-NTAL mAb, were prepared as in Figure 3 and then probed with antiphosphotyrosine mAb (pY) or anti-pY<sup>191</sup>-LAT (pLAT/NTAL) as indicated in the figure. C indicates control; T, treated. (C) HuMCs were challenged for the indicated periods of time, and then the cell extracts were probed using the anti-pY<sup>191</sup>-LAT antibody, other phospho-specific antibodies as indicated in the figure, or Syk to determine loading. (D) Sensitized cells were challenged with either NP-BSA (100 ng/mL), SCF (100 ng/mL), or a combination for the indicated periods of time. The extracted proteins were then probed for the indicated proteins. The blots are representative of up to 4 similar experiments.

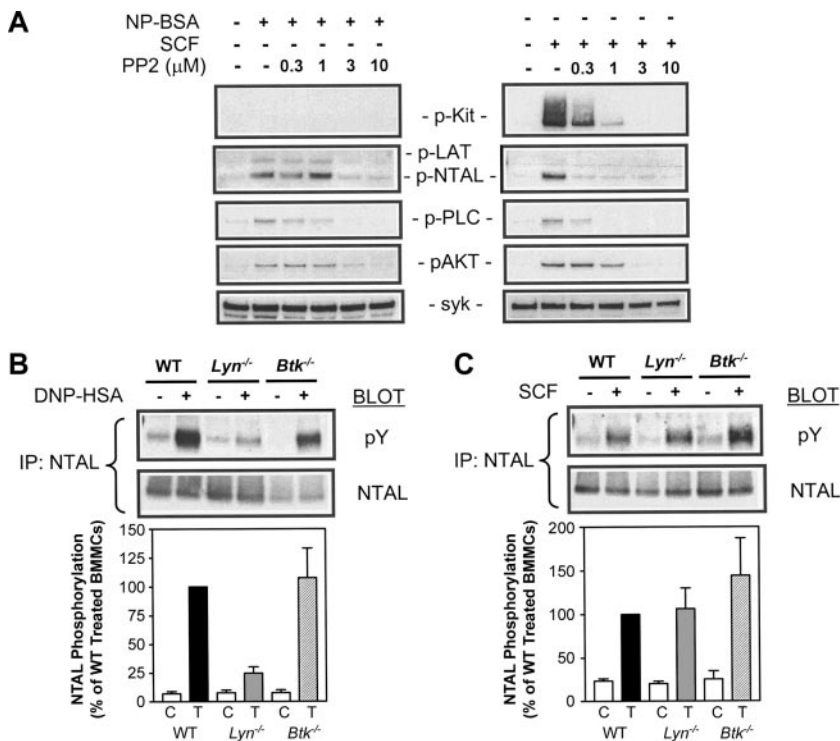


**Figure 6. Effect of PP2 on antigen- and SCF-mediated protein phosphorylation in HuMCs, and antigen- and SCF-mediated NTAL phosphorylation in *Lyn*<sup>-/-</sup> and *Btk*<sup>-/-</sup> BMMCs.** (A) Sensitized HuMCs were triggered via Fc $\epsilon$ RI (NP-BSA, 100 ng/mL) or Kit (SCF, 100 ng/mL) for 60 seconds in the absence or presence of the indicated concentrations of PP2. The extracted proteins were then probed using phospho-specific antibodies, or for Syk as described in Figure 5B. (B-C) Sensitized BMMCs were triggered with (B) DNP-HSA (100 ng/mL) or (C) SCF (100 ng/mL) for 120 seconds, and proteins were extracted under nondenaturing conditions and immunoprecipitated with anti-NTAL mAb. The immunoprecipitates were then probed with antiphosphotyrosine and anti-NTAL mAbs. The gels were then scanned and the data initially normalized to NTAL loading and then calculated as a percentage of the W/T triggered responses. These data are presented in the bar charts. The blots are representative of up to 4 similar experiments and the bar charts are means  $\pm$  SE of  $n = 4$ .

previously described to block Kit activity.<sup>28</sup> In parallel, as was the case with Fc $\epsilon$ RI aggregation (Figure 6A), there was also a complete inhibition of NTAL phosphorylation and downstream responses including phosphorylation of PLC $\gamma$ <sub>1</sub> and AKT. The concentrations of PP2 required to block the Kit-mediated responses were lower than those required to block the Fc $\epsilon$ RI-mediated responses. Thus, although it cannot be ruled out that Src kinases or other kinases may also be involved, these data suggest that Kit kinase activity is required for SCF-mediated phosphorylation of NTAL.

To further investigate the possibility that Kit and Fc $\epsilon$ RI may induce NTAL phosphorylation by the action of different kinases, we examined the relative abilities of SCF and antigen to induce NTAL phosphorylation in mast cells derived from the bone marrow of wild-type (W/T) and *Lyn*<sup>-/-</sup> mice. Previous studies have demonstrated a marked ablation of overall protein tyrosine phosphorylation in response to antigen in *Lyn*<sup>-/-</sup> BMMCs.<sup>19</sup> In addition, *Lyn* appears to be critical for specific Kit-mediated responses.<sup>29</sup> As Tec kinases have also been implicated in mast cell activation<sup>30</sup> and LAT phosphorylation in T cells,<sup>31,32</sup> we also examined SCF- and antigen-dependent NTAL phosphorylation in *Btk*<sup>-/-</sup> BMMCs. *Btk* is the major Tec kinase involved in mast cell activation.<sup>33</sup> Due to the lower magnitude of the SCF response in mouse BMMCs, the increase in NTAL phosphorylation above background in response to SCF could not be detected with the anti-phospho-LAT antibody. Thus, in these and other experiments in which we examined the effects of SCF in mouse BMMCs, it was necessary to immunoprecipitate NTAL and then probe with an antiphosphotyrosine antibody to detect NTAL phosphorylation.

From Figure 6B, it can be seen that the tyrosine phosphorylation of NTAL in response to antigen was substantially inhibited in *Lyn*<sup>-/-</sup> BMMCs but not in BMMCs derived from *Btk*<sup>-/-</sup> mice. In contrast, SCF-induced NTAL phosphorylation was observed in both the *Lyn*<sup>-/-</sup> and *Btk*<sup>-/-</sup> BMMCs (Figure 6C). These results support the conclusion that Fc $\epsilon$ RI and Kit differentially regulate NTAL phosphorylation.

#### RNA interference studies

To determine whether NTAL indeed played a role in Fc $\epsilon$ RI- and Kit-mediated HuMC degranulation, 3 interfering RNA oligonucleotides for NTAL with different sequences were transfected into HuMCs 72 hours prior to activation. Oligonucleotides based on the LAT sequence and oligonucleotides based on the sequence for GFP

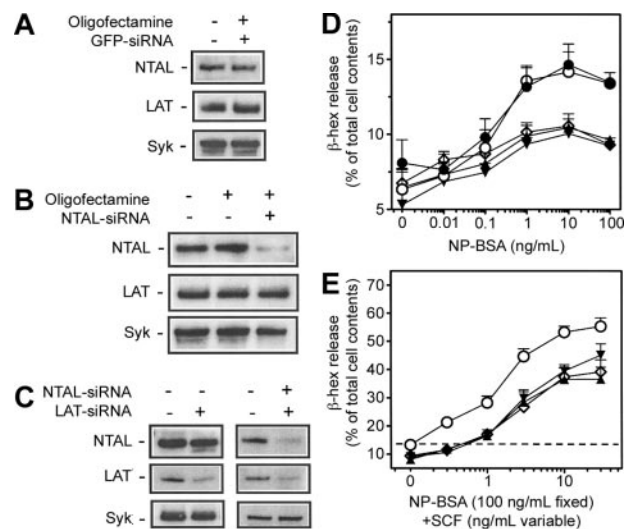


**Figure 7. The effects of siRNA on protein expression and degranulation in HuMCs.** HuMCs were incubated with (A-E) the indicated siRNAs or appropriate controls for a total of 72 hours; then the cells were either processed for (A-C) immunoblot analysis or (D-E) degranulation experiments. Immunoblot analyses for the indicated proteins and  $\beta$ -hex release assays were then conducted as described in Figure 1. The blots are representative of 3 to 4 similar experiments in which NTAL-siRNA induced an average 70% knockdown of NTAL expression, and LAT-siRNA induced an average 61% knockdown of LAT expression. The release data are means  $\pm$  SEM of 4 to 6 separate experiments conducted in duplicate. ● indicates cells alone, no siRNA; ○, GFP-siRNA; ▲, NTAL-siRNA; ▼, LAT-siRNA; and ◇, NTAL + LAT siRNA. (E) The horizontal dashed line represents the antigen response in the absence of siRNA and SCF.

were used as positive and negative controls, respectively. Oligofectamine alone and the GFP siRNA-negative control did not affect the expression of NTAL, LAT, or Syk (Figure 7A). Incubation of the HuMCs with NTAL siRNAs resulted in a specific knockdown of NTAL by approximately 70% (Figure 7B). No differences in expression of either LAT or Syk were observed under these conditions (Figure 7B). Similarly, the LAT siRNAs also resulted in a reduction in LAT expression in the absence of defects in NTAL or Syk expression (Figure 7C). Finally, when siRNAs for NTAL and LAT were added concurrently, the degree of knockdown of the respective proteins was similar to that observed when they were added independently (Figure 7C). Again the expression of Syk was unaffected by these conditions (Figure 7C).

From Figure 7D, it can be seen that there was a significant reduction in the antigen response when the NTAL or LAT siRNAs were either added individually or concurrently to the HuMCs, even at the highest concentration of antigen (100 ng/mL) (NTAL siRNA:  $P < .05$ , compared with GFP siRNA control; LAT siRNA:  $P < .01$ , compared with GFP siRNA control; NTAL + LAT siRNAs:  $P < .05$ , compared with GFP control). However, the combination of NTAL and LAT siRNAs failed to further decrease the antigen response compared with that observed with the siRNAs when added separately. Both NTAL and LAT siRNAs when added separately or concurrently also reduced degranulation in response to SCF when added to sensitized cells in the presence of antigen (Figure 7E). However, they were more effective at low concentrations of SCF (ie, 1-3 ng/mL) (NTAL siRNA:  $P < .01$ , compared with GFP siRNA control; LAT siRNA:  $P < .01$ , compared with GFP siRNA control; NTAL + LAT siRNAs:  $P < .05$ , compared with GFP controls, at an SCF concentration of 3 ng/mL) than at higher SCF concentrations (10-30 ng/mL); although, even at the highest SCF concentration (30 ng/mL), both NTAL ( $P < .01$ , compared with GFP siRNA control) and LAT ( $P < .05$ , compared with GFP siRNA controls) siRNAs still significantly reduced the degranulation response. As with the antigen response, the combination of both NTAL and LAT siRNAs was no more effective at blocking degranulation than when added separately. Taken together, the data demonstrate that both NTAL and LAT are required for optimal degranulation of HuMCs in response to antigen and SCF.

## Discussion

In this paper, we demonstrate that the major small-MW protein that is tyrosine phosphorylated (pp30) following FcεRI aggregation and Kit activation in HuMCs (Figure 1) is NTAL. Furthermore, our studies provide evidence that NTAL phosphorylation may be a central link between the signaling pathways elicited by these receptors, which eventually culminate in human mast cell degranulation. The identification of pp30 as NTAL in HuMCs was based on the comigration of pp30 and NTAL (Figure 2), and immunodepletion studies in which both NTAL and pp30 were effectively depleted from lysates of activated HuMCs using an anti-NTAL antibody (Figure 3). The demonstration of a corresponding small-MW (28 kDa) densely phosphorylated protein in mouse BMMCs (Figure 2), and the phosphorylation of NTAL, upon FcεRI aggregation (also Brdicka et al<sup>14</sup>) and SCF challenge (Figure 5) in these cells suggests that these responses are typical of all nontransformed mast cells and not just restricted to HuMCs.

NTAL is a glycolipid-enriched membrane-associated transmembrane adaptor molecule structurally and functionally similar to

LAT, but, unlike LAT, NTAL is not expressed in resting T cells, but rather in other leukocytes.<sup>14</sup> Within the cytosolic domain of NTAL, there are multiple tyrosine residues that are targets for *Src* and Syk family kinases, thus providing multiple docking sites for SH2-containing signaling molecules, including growth factor receptor-bound protein 2 (Grb2), son of sevenless 1 (Sos1), Grb2-associated binder-1 (Gab1), and c-Cbl.<sup>14</sup> In addition, NTAL has been reported to coimmunoprecipitate with PLCγ<sub>1</sub>, PLCγ<sub>2</sub>, and SLP-65 in a B-cell line,<sup>15</sup> although a previous study failed to find association of PLCγ<sub>1</sub> with phosphorylated NTAL.<sup>14</sup> NTAL therefore appears to be the central transmembrane adaptor protein linking the B-cell receptor (BCR) to B-cell activation,<sup>14,15</sup> whereas LAT plays this role in T-cell receptor (TCR)-mediated T-cell activation.<sup>34</sup>

Our demonstration of NTAL phosphorylation in response to Kit activation is the first report of a growth factor receptor regulating the phosphorylation of one of the major hematopoietic cell transmembrane adaptor proteins, NTAL or LAT. In contrast to FcεRI aggregation, however, Kit induces the phosphorylation of NTAL in the absence of detectable LAT phosphorylation (Figure 5). From studies conducted in mouse BMMCs, it appears that, as in T cells, LAT is the central transmembrane adaptor molecule phosphorylated upon FcεRI aggregation.<sup>35</sup> However, degranulation in response to FcεRI aggregation is not completely knocked out in BMMCs derived from LAT-deficient mice.<sup>36</sup> Thus, both NTAL- and LAT-dependent pathways may be required for maximal degranulation.

This conclusion is supported by our studies using siRNA targeted to NTAL and LAT expression, in which we could obtain a marked, but not complete, knockdown of the expression of these proteins (Figure 7). Parallel studies with siRNA for GFP, and probing for the effects of the oligonucleotides on Syk expression, suggested specific depletion of the targeted molecules. Associated with the knockdown of NTAL and LAT expression, there was a significant reduction in antigen-mediated degranulation (Figure 7), thus both NTAL and LAT appeared to be indispensable for optimal degranulation in response to FcεRI aggregation. There was no additional decrease in degranulation observed when NTAL and LAT siRNAs were added concurrently. This may suggest that these adaptor molecules ultimately regulate a common distal signaling pathway for antigen-mediated degranulation. Both NTAL and LAT siRNAs also reduced the degranulation response due to SCF, however, they were more effective at lower SCF concentrations (ie, 1-3 ng/mL). The reduced inhibition at higher concentrations of SCF (10-30 ng/mL) likely reflects the fact that these proteins were not completely depleted from the HuMCs. Thus, the higher degree of activation of Kit at these concentrations may provide sufficient docking sites on NTAL to initiate degranulation.

Together with the phosphorylation results (Figure 5), the siRNA data support the conclusion that activated Kit and aggregated FcεRI provide synergistic signals for enhanced NTAL phosphorylation. In the absence of FcεRI aggregation, SCF does not induce degranulation, as there is no increase in LAT phosphorylation. When this response is present following FcεRI aggregation, the enhanced NTAL phosphorylation can then induce the potentiation of degranulation.

An explanation for the differential phosphorylation of NTAL and LAT following Kit activation and FcεRI aggregation may be the different kinases used for these responses. Inhibitor studies suggested that the tyrosine phosphorylation of NTAL in FcεRI-activated mast cells appears to be positively regulated via *Src* kinases and Syk and negatively regulated via a PI-3 kinase-dependent pathway (Figure 6). Data obtained with BMMCs

derived from *Lyn*<sup>-/-</sup> mice revealed that the *Src* kinase responsible was primarily *Lyn*. In contrast, these studies also revealed that *Kit* did not require *Lyn* to induce NTAL phosphorylation. PP2 has been previously reported to inhibit *Kit* kinase activity.<sup>28,37</sup> Thus, although it cannot be completely ruled out that other kinases are involved, as PP2 also blocked SCF-mediated autophosphorylation of *Kit* in parallel with SCF-dependent NTAL phosphorylation, both of these responses may be directly mediated by inherent *Kit* kinase activity. Direct phosphorylation of NTAL by *Kit* may also help to explain the lack of observed phosphorylation of LAT in response to *Kit*, especially if LAT was a poor substrate for *Kit* kinase activity.

In conclusion, in this paper, we have demonstrated that the major small-MW protein that is tyrosine phosphorylated after both FcεRI aggregation and *Kit* activation in human mast cells is NTAL and that NTAL appears to be required for both FcεRI- and *Kit*-mediated degranulation. There have been two complementary pathways described to contribute to FcεRI-mediated degranulation

in mouse BMMCs.<sup>17</sup> Although LAT links one of these pathways to the FcεRI, in a manner similar to that observed with the TCR in T cells, the identity of the transmembrane adaptor molecule linking the other signaling pathway is unknown. The ability of NTAL (linker for activated B cells [LAB]) to bind to *Gab1*, *Grb2*, *Sos1*, *c-Cbl*, *PLC-γ1*, and *SLP-65*<sup>14</sup> suggests that NTAL may link the other pathway to the FcεRI in a manner similar to that for BCR activated in B cells. Thus, our data demonstrate the presence of both TCR- and BCR-like signaling pathways in mast cells following FcεRI aggregation.

## Acknowledgments

The authors would like to thank Clifford A. Lowell MD, PhD, Department of Laboratory Medicine, University of California, San Francisco, CA 94143-0134 for providing us with knock-out mice.

## References

1. Metcalfe DD, Baram D, Mekori YA. Mast cells. *Physiol Rev*. 1997;77:1033-1079.
2. Galli SJ. New insights into "the riddle of the mast cells": microenvironmental regulation of mast cell development and phenotypic heterogeneity. *Lab Invest*. 1990;62:5-33.
3. Galli SJ, Tsai M, Wershil BK. The c-kit receptor, stem cell factor, and mast cells: what each is teaching us about the others. *Am J Pathol*. 1993;142:965-974.
4. Bischoff SC, Dahinden CA. C-kit ligand: a unique potentiator of mediator release by human lung mast cells. *J Exp Med*. 1992;175:237-244.
5. Benhamou M, Siraganian R. Protein-tyrosine phosphorylation: an essential early component of FcεRI signalling. *Immunol Today*. 1992;13:195-201.
6. Welham MJ, Schrader JW. Steel factor-induced tyrosine phosphorylation in murine mast cells: common elements with IL-3 induced signal transduction pathways. *J Immunol*. 1992;149:2772-2783.
7. Benhamou M, Ryba NJP, Kihara H, et al. Protein-tyrosine kinase p72syk in high affinity IgE receptor signalling. *J Biol Chem*. 1993;268:23318-23324.
8. Jouvin MHE, Adamczewski M, Numerof R, et al. Differential control of the tyrosine kinases *lyn* and *syk* by the two signalling chains of the high affinity immunoglobulin E receptor. *J Biol Chem*. 1994;269:5918-5925.
9. Rivera J. Molecular adapters in Fc(epsilon)RI signaling and the allergic response. *Curr Opin Immunol*. 2002;14:688-693.
10. Yarden Y, Kuang WJ, Yang-Feng T, et al. Human proto-oncogene c-kit: a new cell surface receptor tyrosine kinase for an unidentified ligand. *Embo J*. 1987;6:3341-3351.
11. Majumder S, Brown K, Qiu FH, et al. C-kit protein, a transmembrane kinase: identification in tissues and characterization. *Mol Cell Biol*. 1988;8:4896-4903.
12. Linnekin D. Early signaling pathways activated by c-kit in hematopoietic cells. *Int J Biochem Cell Biol*. 1999;31:1053-1074.
13. Tkaczyk C, Metcalfe DD, Giffillan AM. Determination of protein phosphorylation in FcεRI-activated human mast cells by immunoblot analysis requires protein extraction under denaturing conditions. *J Immunol Met*. 2002;268:239-243.
14. Brdicka T, Imrich M, Angelisova P, et al. Non-T cell activation linker (NTAL): a transmembrane adaptor protein involved in immunoreceptor signaling. *J Exp Med*. 2002;196:1617-1626.
15. Janssen E, Zhu M, Zhang W, et al. LAB: a new transmembrane-associated adaptor molecule in B cell activation. *Nat Immunol*. 2003;4:117-123.
16. Kirshenbaum AS, Kessler SW, Goff JP, et al. Demonstration that human mast cells arise from a progenitor cell population that is CD34<sup>+</sup>, c-kit<sup>+</sup> and expresses aminopeptidase N (CD13). *Blood*. 1999;94:2333-2342.
17. Parravicini V, Gadina M, Kovarova M, et al. Fyn kinase initiates complementary signals required for IgE-dependent mast cell degranulation. *Nat Immunol*. 2002;3:741-748.
18. Okayama Y, Kirshenbaum AS, Metcalfe DD. Expression of a functional high-affinity IgG receptor, FcγRI, on human mast cells: up-regulation by IFN-γ. *J Immunol*. 2000;164:4332-4339.
19. Kawakami Y, Kitaura J, Satterthwaite AB, et al. Redundant and opposing functions of two tyrosine kinases, *Btk* and *lyn*, in mast cell activation. *J Immunol*. 2000;165:1210-1219.
20. Chaves-Dias C, Hundley TR, Giffillan AM, et al. Induction of telomerase activity during development of human mast cells from peripheral blood CD34<sup>+</sup> cells: comparisons with tumor mast-cell lines. *J Immunol*. 2001;166:6647-6656.
21. Yamashita T, Kairiyama L, Araki M, et al. Evidence for involvement of two isoforms of *syk* protein-tyrosine kinase in signal transduction through the high affinity IgE receptor on rat basophilic leukemia cells. *J Biochem*. 1998;123:1199-1207.
22. Minoguchi K, Benhamou M, Swaim WD, et al. Activation of protein tyrosine kinase p72syk by FcεRI aggregation in rat basophilic leukemia cells: p72syk is a minor component but the major protein tyrosine kinase of pp72. *J Biol Chem*. 1994;269:16902-16908.
23. Pivniouk VI, Martin TR, Lu-Kuo JM, et al. SLP-76 deficiency impairs signaling via the high-affinity IgE receptor in mast cells. *J Clin Invest*. 1999;103:1737-1743.
24. Beaven MA, Baumgartner RA. Downstream signals initiated in mast cells by FcεRI and other receptors. *Curr Opin Immunol*. 1996;8:766-772.
25. Barker SA, Caldwell KK, Pfeiffer JR, et al. Wortmannin-sensitive phosphorylation, translocation, and activation of PLC-γ1, but not PLC-γ2, in antigen-stimulated RBL-2H3 mast cells. *Mol Biol Cell*. 1998;9:1145-1158.
26. Hanke JH, Gardner JP, Dow RL, et al. Discovery of a novel, potent, and *src* family-selective tyrosine kinase inhibitor. *J Biol Chem*. 1996;271:695-701.
27. Oliver JM, Burg DL, Wilson BS, et al. Inhibition of mast cell FcεRI-mediated signaling and effector function by the *syk*-selective inhibitor, piceatanol. *J Biol Chem*. 1994;269:29697-29703.
28. Tatton L, Morley JM, Chopra R, et al. The *Src*-selective inhibitor PP1 also inhibits *Kit* and *Bcr-Abl* tyrosine kinases. *J Biol Chem*. 2003;278:4847-4853.
29. O'Laughlin-Bunner B, Radosevic N, Taylor ML, et al. *Lyn* is required for normal stem cell factor-induced proliferation and chemotaxis of primary hematopoietic cells. *Blood*. 2001;98:343-350.
30. Kawakami Y, Yao L, Tashiro M, et al. Activation and interaction with protein kinase C of a cytoplasmic tyrosine kinase, *Itk/Tsk/Emt*, on FcεRI cross-linking on mast cells. *J Immunol*. 1995;155:3556-3562.
31. Bunnell SC, Diehn M, Yaffe MB, et al. Biochemical interactions integrating *Itk* with the T cell receptor initiated signaling cascade. *J Biol Chem*. 2000;275:2219-2230.
32. Ching KA, Grasis JA, Taylor P, et al. TCR/CD3-induced activation and binding of *Erm1/Itk* to linker of activated T cell complexes: requirement for the *src* homology 2 domain. *J Immunol*. 2000;165:256-262.
33. Hata D, Kawakami Y, Inagaki N, et al. Involvement of *Bru-1*'s tyrosine kinase in FcεRI-dependent mast cell degranulation and cytokine production. *J Exp Med*. 1998;187:1235-1247.
34. Samelson LE. Signal transduction mediated by T cell antigen receptor: the role of adapter proteins. *Annu Rev Immunol*. 2002;20:371-394.
35. Saitoh S, Odum S, Gomez G, et al. The four distal tyrosines are required for LAT-dependent signaling in FcεRI-mediated mast cell activation. *J Exp Med*. 2003;198:831-843.
36. Saitoh S, Arudchandran R, Manetz TS, et al. LAT is essential for FcεRI-mediated mast cell activation. *Immunity*. 2000;12:525-535.
37. Endo T, Odb A, Satoh I, et al. Stem cell factor protects c-kit<sup>+</sup> human primary erythroid cells from apoptosis. *Exp Hematol*. 2001;29:833-841.